Optical diffraction and high-energy features in three-dimensional photonic crystals

F. García-Santamaría,[1,*] J. F. Galisteo-López,[2] P. V. Braun,[1] and C. López[2]

[1]*Department of Materials Science and Engineering, Frederick Seitz Materials Research Laboratory and Beckman Institute,*
University of Illinois at Urbana-Champaign, Urbana, Illinois 61801, USA
[2]*Instituto de Ciencia de Materiales de Madrid (CSIC), C/ Sor Juana Inés de la Cruz 3, 28049 Madrid, Spain*

We provide a band-structure-based interpretation of the diffraction phenomena observed in three-dimensional photonic crystals. Qualitative and quantitative information about these patterns is obtained in a simple manner from the band structure. Our conclusions and experimental results explain phenomena occurring at frequencies above the first stop band that were not previously understood. Optical features observed in transmission spectra from opaline photonic crystals are now clarified by relating them to diffraction phenomena. We also observe an intriguing change in the diffraction pattern symmetry when the photonic-crystal refractive-index contrast is modified.

Understanding the optical response of photonic crystals[1] (PhCs) in the high-energy region of the spectra (above the first stop band) has paramount importance since that region is where many of the most appealing phenomena occur. Some examples are anomalous refraction,[2–4] small group-velocity eigenmodes,[5] and, in some specific lattices, the opening of a complete photonic band gap.[6] Although all these effects are being extensively studied in two-dimensional (2D) PhCs, the high-energy region of the spectra is just beginning to be explored in 3D systems. Similarly, diffraction patterns in 3D PhCs have been scarcely investigated and experiments performed have generally been explained with a single-scattering model (SSM).[7] It is known that this model must fail for an increasing refractive-index contrast. But, to date, a more comprehensive theoretical study has been too complex due to the many bands present at high energies. Also, experimentally, very high-quality samples were needed to obtain reliable spectra.

This article shows how the high-energy features and the diffraction phenomena are closely related. It illustrates how fundamental information about diffraction patterns from PhCs can be extracted from the band structure and clarifies the physics of this phenomenon, something that a numerical method alone does not do.[5] Due to the nature of the band-structure calculations, the results take full account of the refractive-index contrast and dimensionality of the system. This gives us a theoretical basis to account for the experimentally observed behavior of the onset of diffraction that the SSM could not explain. Our results illuminate important previously unexplained features found in the optical transmission spectra of opaline systems. Finally, we also find evidence showing that the symmetry of diffraction patterns in opals can be affected by different values of the refractive-index contrast $\delta = |n_s - n_h|$, where n_s and n_h are the building-block and host dielectric refractive indices, respectively.

Diffraction patterns are built by a constructive interference of light scattered in directions other than the incident and specular ones. In a PhC, the wave vector can take the form of $\boldsymbol{k}_i + \boldsymbol{G}$, where $\boldsymbol{k}_i$ is the initial wave vector and $\boldsymbol{G}$ denotes any reciprocal lattice vector. In the particular case of normal incidence, the parallel component of $\boldsymbol{k}_i$ is the null

vector; however, the many possible values of $\boldsymbol{G}$ still provide the photon wave vector with a parallel component. In the external medium, the angle of the exiting beam with respect to the normal is given by $\sin(\varphi) = k_\parallel / k_{\mathrm{out}}$, where $k_\parallel$ is the parallel component of the wave vector and is a conserved quantity[8] and k_{out} is the modulus of the wave vector in the external medium. This imposes the following condition onto the wave-vector modulus out of the PhC to observe the diffraction patterns: $k_{\mathrm{out}} \geq k_\parallel$. As an example, Fig. 1 shows the reciprocal lattice of a hexagonal array. In particular, if light propagates in the ΓM direction any possible value for $k_\parallel$ inside the PhC must take the form of $m 2\pi/a$. Here m is an integer number (the diffraction order) and a is the lattice parameter. Alternatively, the condition of having a large enough wave vector to observe diffraction patterns can be expressed as $a/\lambda \geq m/n$, where λ and n are the wavelength and the refractive index of the external medium, respectively. It is interesting to notice that this equation is the same that would be obtained for a grating with a periodicity of a. All the previous arguments lead to a first necessary condition to project the diffraction pattern out of the PhC. But in contrast with gratings, PhCs impose a second condition due to their dimensionality as photons must propagate through the PhC. To obtain a diffraction pattern from photons that propagate normally to the surface of the PhC, the photons must couple with bands (eigenstates) that provide them with a non-null $k_\parallel$. This occurs when bands folded back into the first Brillouin zone (BZ) by reciprocal lattice (RL) vectors not collinear with $\boldsymbol{k}_i$ are available.[5] Conversely, bands folded back by RL vectors collinear with $\boldsymbol{k}_i$ will transmit light only in the forward direction. The former bands are only present on media periodically structured in 2D or 3D while the latter are present in 1D PhCs as well (i.e., Bragg stacks). Thus, the second requirement to observe a diffraction pattern from a PhC is the existence of a Bloch mode created by a noncollinear RL vector to which photons may couple. In general, for low energies (below the first stop band) only linear bands are available. This means that the second condition also imposes a minimum on the photon energy to produce diffraction patterns. Consequently, it is necessary to interpret the
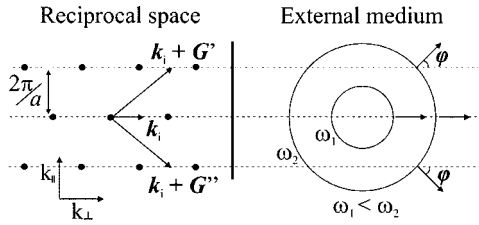
FIG. 1. Reciprocal lattice of a hexagonal 2D PhC (solid dots on the left) and equifrequency surfaces in the external medium for two different photon energies (right). The photon wave vector (k_i) can take within the PhC any value k_i+G for any reciprocal lattice vector. For low frequencies (ω_1), only a single beam normal to the surface of the PhC is projected out. For high enough frequencies (ω_2) photons exiting the PhC with an angle φ respect to the normal can be observed.

FIG. 2. (a) Band structure in the ΓL direction for a fcc structure made of touching spheres ($n_s=1.4597$) in a host dielectric ($n_h=1.4598$). Bands have been grouped according to the direction of the *RL* vector that folds them back into the first BZ. (b) Same as (a) with $n_s=1.59$ and $n_h=1.00$ (PS spheres in air). The arrows indicate the onset of the two sets of diffraction patterns.

diffraction phenomena in terms of photonic bands and to identify the modes responsible for the diffraction. Given a specific PhC, a good starting point is to compare its band structure to that of a PhC with the same lattice and average dielectric constant but a negligible δ. The latter is the case in which the PhC behaves as a homogeneous dielectric.

A face-centered-cubic (fcc) arrangement of close-packed spheres will be used as a model system. However, the conclusions and approaches presented here can be generalized for other configurations. The fcc lattice of close-packed spheres is a generally accessible 3D photonic crystal of great interest for which the optical features are not yet fully understood.[9–11] These crystals usually present {111} planes parallel to the crystal surface[12] and the direction normal to these planes (also called ΓL) has been preferentially studied. As explained before, the first condition that must be satisfied to observe the diffraction patterns is that $k_{out} \geqslant k_\parallel$. From the reciprocal lattice in the ΓL direction we can deduce the following equation that predicts for which energies and lattice parameters that condition is satisfied:

$$\frac{a}{\lambda} \geqslant m\frac{\sqrt{2}}{n}\left[1 + \frac{(2s-1)^2}{3}\right]^{1/2},$$

where s and m are two integer numbers which represent the set of diffraction spots and the diffraction order, respectively. Therefore, the lowest energy that satisfies this condition is $a/\lambda=1.633/n$ ($m=s=1$). Another set of diffraction spots appears for $a/\lambda \geqslant 2.828/n$ ($m=1$, $s=2$). This second set should not be mistaken for a higher diffraction order of the first set as it appears was assumed by some authors.[13,14]

To understand the implications of the second condition the bands created by noncollinear RL vectors in the PhC band structure must be identified. Figure 2(a) is the band structure along the ΓL direction in reciprocal space for the case of a system with very low refractive-index contrast ($n_s=1.4597$ and $n_h=1.4598$). Four groups of bands with different degrees of degeneracy can be observed for this range of energies corresponding to different RL folding vectors. Filled symbols correspond to those bands showing a linear dependence on frequency. Light coupled to these bands will propagate in the forward direction. Open symbols correspond to three different groups of bands which are folded
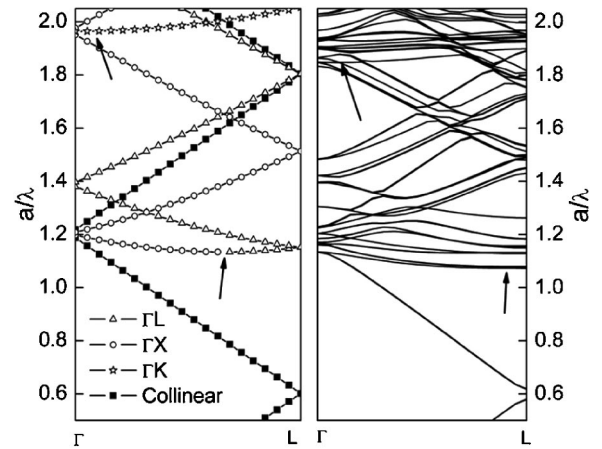
back in the first BZ by reciprocal lattice vectors in the ΓL, ΓX, and ΓK directions. These three directions are all noncollinear with k_i since those indicated as ΓL are coming from {111} planes other than the normal to k_i. The ΓL and ΓX groups will be responsible for the first set of diffraction spots appearing for $a/\lambda \geqslant 1.12$. The ΓK group will cause the second set of spots for $a/\lambda \geqslant 1.94$.

Figure 2(b) shows the band structure[15] of a fcc array of touching polystyrene (PS) spheres in air. While this PhC has the same average refractive index it shows very important differences when compared with the quasihomogeneous crystal shown in Fig. 2(a). Apart from the widely reported[16] opening of a pseudogap at low energies ($a/\lambda=0.61$) in the ΓL direction, increasing δ leads to a strong interaction among the high-energy bands. The degeneracy of the bands begins to lift and some of them split due to anticrossings. The frequency at which diffraction begins is redshifted. Indeed, the first set of spots is now expected for $a/\lambda \geqslant 1.08$ and the second set for $a/\lambda \geqslant 1.85$.

The results obtained from the band structure are now compared with experimental data. The study of the angle at which the beams are diffracted out of the sample versus the photon frequency will not provide new information since that behavior is identical to that of a diffraction grating: $\sin(\varphi)=k_\parallel/k_{out}$. However, the onset of the diffraction spots must also be satisfied by the condition imposed by the dimensionality of the PhC. For this reason, the onset of different sets of diffraction spots at various energies is a meaningful experiment. Diffraction experiments were performed with light from a tunable nanosecond pulsed optical parametric oscillator. The samples are thin opals ($\sim$30 layers) assembled from PS spheres on a glass substrate ($n=1.53$) following a published method[17] based on vertical deposition techniques.[18] The light passes first through the sample and then the substrate. This configuration allows the observation of diffraction patterns in the sample itself; for the lowest energies (large diffraction angle), the diffracted beams un-
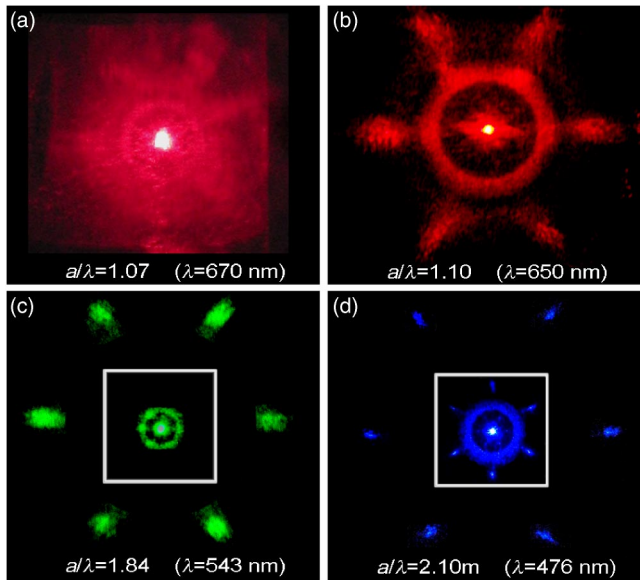
FIG. 3. (Color online) Diffraction patterns generated by opals made of (a),(b) 505 and (c),(d) 705 nm PS microspheres. The first two pictures are taken on the sample while the latter two include both the sample (inset) and the diffraction pattern projected on a screen. Notice that diffraction pattern shown in the sample at (d) is rotated by 30° with respect to the spots projected on the screen.

dergo total internal reflection (TIR) on the opposite side of the substrate and project back on the opal, which acts as a screen. For higher energies (smaller diffraction angle), TIR does not occur and the pattern is projected on an external screen. A similar configuration for a 2D grating is described in Ref. 13. Figure 3(a) shows the laser light with energy $a/\lambda=1.07$ incident in the ΓL direction on the sample. This energy is just below the first band capable of diffracting and therefore no pattern is observed. For $a/\lambda=1.10$ [Fig. 3(b)] the diffraction pattern is already observed on the sample. When $a/\lambda>1.63$ the diffracted beams exit the sample and are projected on a screen [Fig. 3(c)]. This is for geometric reasons only as TIR is avoided at this energy for the refractive index of the substrate. For $a/\lambda>1.85$ the first set of spots is projected on the screen while the second set still undergoes TIR and thus is observed on the sample [Fig. 3(d)]. Increasing the energy will eventually allow the projection of both first and second sets of spots on the screen. In the particular case of PS opals on a glass substrate, the conditions imposed by the band structure and the grating equation are satisfied for very similar photon energies.

In the case of diffraction patterns that undergo total internal reflection in the substrate it may be difficult or not possible to observe the diffracted beams [Fig. 4(a)]. A simple way to project those beams out of the substrate is to change the geometry to avoid TIR. The attachment of a glass hemisphere to the back of the substrate is a possible geometry that enables observation of the diffraction pattern on an external screen. Figure 4(b) shows such a setup in which the hemisphere is glued to the substrate with a droplet of glycerol.

The band minima determining the onset of diffraction in a certain direction may happen to be saddle points and not absolute minima. As a consequence, increasing the external
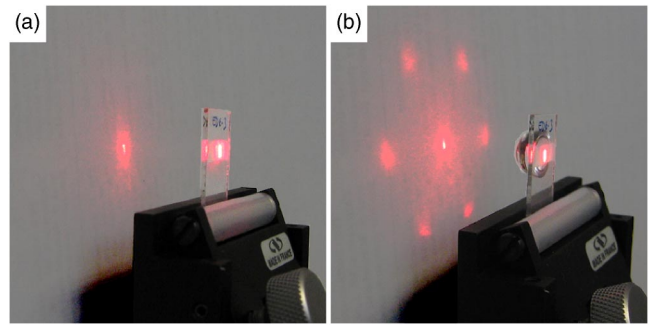

FIG. 4. (Color online) (a) For certain frequencies the diffracted beams may undergo total internal reflection in the sample substrate. (b) A glass hemisphere attached to the back of the glass substrate enables the diffracted beams to project out of the substrate.

angle of incidence (θ) may lead to reduction of onset energy. This is the case of the ΓL direction on a fcc lattice. Calculations extracted from the band structure show (Fig. 5) that, for an opal made of poly(methyl methacrylate) (PMMA) spheres ($n_s=1.50$), the diffraction pattern at $\theta=0°$ (ΓL) is expected for $a/\lambda\geq1.14$. However, as θ increases, the minimum energy at which the diffraction pattern can be observed decreases. The behavior depends on the crystallographic direction under study, the $LK(U)$ (Ref. 19) and the LW directions in this case. The results are compared to the behavior of a 2D grating with the same lattice parameter on a glass substrate. To experimentally illustrate this, an opal made of 334 nm PMMA spheres was fabricated and illuminated with a 476 nm laser beam which makes $a/\lambda=0.99$. Both the LW and the $LK(U)$ directions[17] were probed. For $\theta=0°$ no diffraction pattern was observed. For $\theta=30°$, the crosshairs in Fig. 5, this photon energy is sufficient to form diffraction patterns whose symmetry depends on the direction (insets in Fig. 5). As predicted, no diffraction patterns were observed
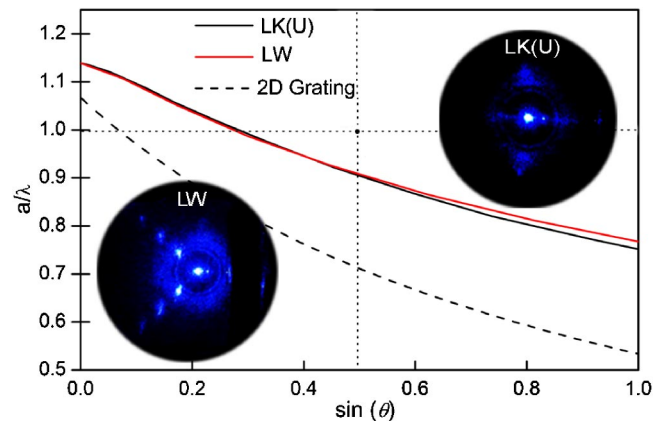

FIG. 5. (Color online) Onset of diffraction extracted from band-structure calculations as a function of normalized frequency and the external angle of incidence along the $LK(U)$ (black line) and LW [dark gray (red) line] directions for PMMA spheres ($n_s=1.50$). Dashed line shows the values predicted by the 2D grating equation on a glass substrate ($n=1.53$). The insets show the diffraction patterns when a 476 nm laser impinges at 30° off normal toward the $LK(U)$ and the LW directions. The crosshairs indicate the frequency and angle for the experiment.
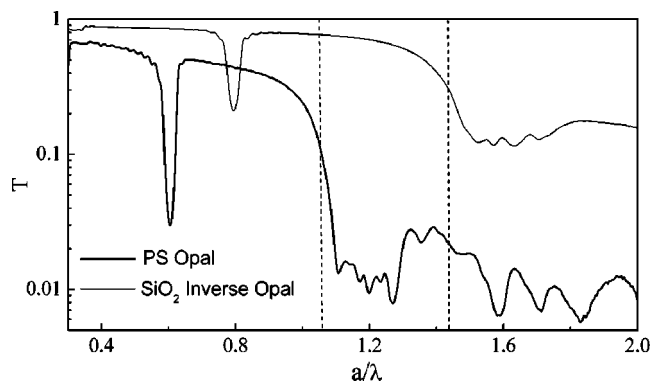
FIG. 6. Transmittance spectra in the ΓL direction of an opal made of 705 nm PS spheres (thick line) and its inverted replica made of silica (thin line) collected with a $4\times$ objective (numerical aperture $=0.1$). Dashed vertical lines depict the energy onset of the sixth band for the direct and the inverse opal.

FIG. 7. (Color online) Diffraction patterns generated by opals made of 705 nm diameter PS microspheres with 70% of the pore volume loaded with SiO_2. The pattern is projected on an external screen using $\lambda = 500$ (a) and 530 nm (b).

for energies and angles below the onset calculated from the band structure.

The presence of bands that scatter light in nonforward directions has obvious effects on the optical spectra of photonic crystals. When diffraction is projected out of the PhC, an intense drop in forward transmission is expected due to the energy imparted to diffracting modes. Transmission dips must also occur over energies where modes causing forward propagation are not available even if other bands are present. Therefore, identifying the latter modes in the band structure is necessary to understand the optical spectra.

Artificial opals are an excellent test bench. Through recent improvements in sample quality[9–11] the high-energy optical spectra at normal incidence can now be studied, but are not fully understood. Figure 6 shows the transmittance spectra of an opal made of PS spheres and its inverse replica made of silica.[20] These samples have the same lattice constant and symmetry but a different band structure. Both samples are on a glass slide and, therefore, the grating equation condition is satisfied for the same energy. However, in the case of the opal and inverse opal, the existence of Bloch modes responsible for diffraction occurs at different energies and so does the diffraction onset. This proves that diffraction patterns are not a 2D effect mainly determined by the first layer as suggested in Ref. 9. As predicted, a drastic drop of transmittance is observed in both cases for the energy at which diffraction begins (depicted as a vertical dashed line). In Ref. 11 this explanation for the transmittance drop was explicitly ruled out since the authors disregarded the fact that diffracted beams, although not extracted out of the opal-substrate system, were present in the glass substrate. Diffraction was only expected at higher energies ($a/\lambda \geq 1.633$) and thus it was concluded that the transmission drop was not related to the diffraction.

A relationship between abrupt oscillations in the spectra and the energies where forward-propagating bands undergo anticrossings and splitting at the edge of the BZ was pointed out in Ref. 10. Nevertheless, a full explanation for these transmission dips was not provided since no depletion in the density of states could be found to account for the transmissi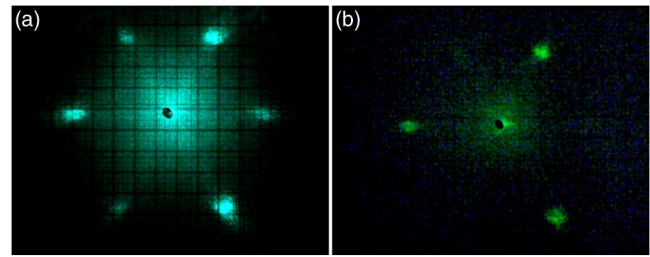on drops. However, as we explain, light collected in forward-transmission probes only those modes that allow forward propagation, while photons coupling to other modes are not collected. Under these circumstances, transmission dips are indeed understood when the spectra and band structures shown in Ref. 10 are compared.

The SSM predicts for a fcc lattice a diffraction pattern consisting of three spots with a C_3 symmetry for incidence normal to the {111} planes.[7] Such a pattern was reported by authors working close to index-matching condition or with crystals formed with a very low number of layers (≤ 3).[7,21] In all our experiments with PS, PMMA, and silica (not shown here) opals, the diffraction patterns showed six spots with a C_6 symmetry.[14] To recreate a low-index-contrast situation, an opal made of 705 nm PS spheres was loaded with silica by means of chemical vapor deposition.[22] The diffraction pattern from this sample showed three spots clearly brighter than the other three, reproducing results reported in the literature. Figure 7 shows examples of these patterns projected on an external screen at two different wavelengths. The intensity distribution indicates that our samples have a strong tendency to be fcc as opposed to random or hexagonal close-packed lattices. Arrangements of close-packed spheres other than the fcc lattice should always lead to a C_6 symmetry diffraction pattern. A challenging question remains as to why the diffraction patterns observed in opals with high and low δ are different. Since for the former, the SSM is inadequate, such a study may require the calculation of the coupling coefficients[3] for bands causing diffraction and more detailed 3D equifrequency surfaces.

To summarize, we provided an explanation for the diffraction patterns in PhCs based on the coupling of incoming light with Bloch modes in the band structure. This interpretation accounts for the onset of diffraction that the SSM failed to predict. The effects of diffraction patterns on optical spectra have been discussed and the conclusions supported by experimental data. Features in the transmission spectra at high energy have been clarified and experimental evidence that relates the diffraction pattern symmetry to δ has been shown.

*Corresponding author. Email address: floren@uiuc.edu

[1] E. Yablonovitch, Phys. Rev. Lett. **58**, 2059 (1987); S. John, *ibid.* **58**, 2486 (1987).

[2] S. Y. Lin, V. M. Hietala, L. Wang, and E. D. Jones, Opt. Lett. **21**, 1771 (1996); H. Kosaka, T. Kawashima, A. Tomita, M. Notomi, T. Tamamura, T. Sato, and S. Kawakami, Phys. Rev. B **58**, R10 096 (1998); M. Notomi, *ibid.* **62**, 10 696 (2000).

[3] T. Ochiai and J. Sánchez-Dehesa, Phys. Rev. B **64**, 245113 (2001).

[4] T. Prasad, V. Colvin, and D. Mittleman, Phys. Rev. B **67**, 165103 (2003).

[5] K. Sakoda, *Optical Properties of Photonic Crystals* (Springer-Verlag, Berlin, 2001); C. López, Adv. Mater. (Weinheim, Ger.) **15**, 1679 (2003).

[6] A. Blanco, E. Chomski, S. Grabtchak, M. Ibisate, S. John, S. W. Leonard, C. López, F. Meseguer, H. Míguez, J. P. Mondia, G. A. Ozin, O. Toader, and H. M. van Driel, Nature (London) **405**, 437 (2000).

[7] R. M. Amos, J. G. Rarity, P. R. Tapster, T. J. Shepherd, and S. C. Kitson, Phys. Rev. E **61**, 2929 (2000).

[8] T. Baba and M. Nakamura, IEEE J. Quantum Electron. **38**, 909 (2002).

[9] K. Wostyn, Y. X. Zhao, B. Yee, K. Clays, A. Persoons, G. de Schaetzen, and L. Hellemans, J. Chem. Phys. **118**, 10752 (2003).

[10] J. F. Galisteo-López and C. López, Phys. Rev. B **70**, 035108 (2004).

[11] H. Míguez, V. Kitaev, and G. A. Ozin, Appl. Phys. Lett. **84**, 1239 (2004).

[12] H. Míguez, F. Meseguer, C. López, A. Mifsud, J. S. Moya, and L. Vázquez, Langmuir **13**, 6009 (1997).

[13] T. Yamasaki and T. Tsutsui, Jpn. J. Appl. Phys., Part 1 **38**, 5916 (1999).

[14] L. M. Goldenberg, J. Wagner, J. Stumpe, B. R. Paulke, and E. Gornitz, Langmuir **18**, 3319 (2002).

[15] Band-structure calculations were performed using freeware developed at MIT [S. G. Johnson and J. D. Joannopoulos, Opt. Express **8**, 173 (2001)].

[16] V. N. Astratov, Y. A. Vlasov, O. Z. Karimov, A. A. Kaplyanskii, Y. G. Musikhin, N. A. Bert, V. N. Bogomolov, and A. V. Prokofiev, Phys. Lett. A **222**, 349 (1996).

[17] J. F. Galisteo-López, E. Palacios-Lidón, E. Castillo-Martínez, and C. López, Phys. Rev. B **68**, 115109 (2003).

[18] P. Jiang, J. F. Bertone, K. S. Hwang, and V. L. Colvin, Chem. Mater. **11**, 2132 (1999).

[19] These two directions have nearly identical band structure for the energy range of interest.

[20] The inverse opal was fabricated following E. Palacios-Lidón, J. F. Galisteo-López, B. H. Juárez, and C. López, Adv. Mater. (Weinheim, Ger.) **16**, 341 (2004).

[21] L. M. Goldenberg, J. Wagner, J. Stumpe, B. R. Paulke, and E. Gornitz, Physica E (Amsterdam) **17**, 433 (2003).

[22] H. Míguez, N. Tetreault, B. Hatton, S. M. Yang, D. Perovic, and G. A. Ozin, Chem. Commun. (Cambridge) **2002**, 2736.